Published: 12th May 2026

ANACHEM JOURNAL
ISSN: 2006-5221 (Online)

TETRAIMINE DIRUTHENIUM COMPLEX: SYNTHESIS, CHARACTERIZATION, ANTIMICROBIAL ACTIVITY AND SARS-COV-2 MOLECULAR DOCKING STUDIES

***[1]Omosun N. N., [1]Okwunodulu F. U., [1]Igwe A. O., and [1]Otuokere I. E.**

[1]Department of Pure and Industrial Chemistry, Michael Okpara University of Agriculture, Umudike, Abia State, Nigeria.
*Corresponding author's e-mail: omosun.nike@mouau.edu.ng
DOI: https://doi.org/10.5281/zenodo.20129841

ABSTRACT

The synthesis, spectroscopic, and biological activity of a new dinuclear ruthenium complex containing a biphenyl spacer and four imine functionalities are reported. 4,4' Tetrakis(methaneylylidene)tetraphenol ligand was obtained *via* a condensation reaction of 4-hydroxybenzaldehyde and 3,3'-diaminobenzidine. The coordination of the tetraimine *N,N* donor Schiff base ligands with cis-dichlorobis(2,2' bipyridine) ruthenium resulted in the formation of a novel tetraimine diruthenium complex. The ligand and the diruthenium complex were characterized using various analytical techniques, including ^{1}H NMR, FT-IR spectroscopy, and mass spectrometry. The antimicrobial activity of the free tetraimine ligand and its diruthenium complex was evaluated against *Candida albicans, Escherichia coli, Staphylococcus aureus, Proteus vulgaris, and Streptococcus pyogenes*, and was compared with that of its monometallic congener. Zone of inhibition measurements demonstrated notable antimicrobial properties, indicating its potential for further therapeutic application. In addition, molecular docking studies were conducted to investigate interactions between the tetraimine ruthenium complex and SARS-CoV-2 nonstructural protein receptors. The most favorable binding conformation showed significant hydrophobic interactions and an affinity energy of –18.35 kcal/mol, suggesting strong interactions between the complex and key residues of the viral proteins. Among all tested compounds, the dinuclear complex gave the highest antimicrobial activity. These findings show the potential of the tetraimine diruthenium complex as a promising antimicrobial agent and inhibitor of SARS-CoV-2, a highly transmissible human pathogen.
Keywords: Antimicrobial activity; Metal complex; Schiff base; Spectroscopy.

1.0. Introduction

Infectious microbial diseases remain a major global health concern, prompting researchers and healthcare professionals to prioritize the development of effective treatment strategies. The situation has been intensified by the rapid emergence of drug-resistant pathogens (Dini, 2026). Addressing this growing resistance requires continuous exploration of innovative therapeutic approaches and advanced drug-design strategies. Among these approaches, metal-based drugs have emerged as a promising and relatively novel class of antimicrobial agents with significant potential for managing infectious diseases (Ahmed et al., 2024; Clemente et al., 2018). Medicinal inorganic chemistry offers distinct advantages in therapeutic design that are not easily achievable with purely organic compounds. In particular, transition metals have gained attention as viable alternatives to traditional antibacterial agents (Waters et al., 2023). The versatility of transition metals reflected in their multiple coordination numbers and

geometries, variable redox states, diverse thermodynamic and kinetic properties, and the intrinsic characteristics of both the metal center and its associated ligands provides medicinal chemists with a broad range of chemical reactivities to exploit (Govender et al., 2012). Within this field, metal complexes incorporating imine ligands and their derivatives represent a particularly promising area of study. Their distinctive coordination behavior with various metal ions enhances their potential for diverse biomedical applications (Antony & Patil, 2024).

Schiff bases are formed through a condensation reaction between primary amines and carbonyl compounds, in which the carbonyl group (C=O) is converted into an imine or azomethine group (–C=N–) (Balachandran et al., 2024). Since their discovery by Hugo Schiff, these compounds have remained highly significant to scientists and researchers because of their broad range of applications across various fields. The imine linkage in Schiff base molecules is a key structural feature responsible for their wide spectrum of biological activities. These include analgesic (More et al., 2022), anticancer (Babgi et al., 2021), antimicrobial, antitumor (Iacopetta et al., 2021), antioxidant, antiviral (Jean-Baptiste *et al.,* 2017) and anti-inflammatory effects (Kathiresan et al., 2017). Beyond their pharmacological relevance, Schiff bases are also employed as chemosensors and in catalytic applications (Afrin et al., 2018).

Tetraimine ligands are characterized by the presence of four exocyclic imine groups, which enhance their σ-donating ability and π-accepting capacity. Additionally, the stereoelectronic properties of substituents attached to the imine moiety play a crucial role in influencing their coordination behavior and reactivity (Gonzalez-Oñate et al., 2026). Metal-based Schiff base complexes have attracted particular attention due to their diverse and promising roles as biological agents (Catalano et al., 2021; Gaber et al., 2021). In particular, di- and polynuclear transition metal complexes of Schiff base derivatives continue to attract significant research interest due to their diverse applications. These complexes offer key components in the development of advanced materials. Polynuclear complexes often offer superior stability and activity, improved structural control and properties over their monometallic congeners. They are also widely utilized as structural building blocks in the construction of metallo-supramolecular architectures (Nastasi et al., 2022).

Herein, we describe the synthesis of a dinuclear homonuclear ruthenium complex. This was achieved using a suitable bidentate single-frame electron-rich, conformationally rigid biphenyl spacer donor ligand. This ligand is designed to chelate two discrete metal centres with two pyridyl groups via the tetraimine nitrogen donor atoms. In this perspective, the facile synthesis of the Schiff base ligand was through the simple condensation of 4-hydroxybenzaldehyde and 3,3'-diaminobenzidine to produce A 4,4' tetrakis(methaneylylidene))tetraphenol ligand A (Scheme 1). The ligand A was further reacted with cis-dichlorobis(2,2'bipyridine)ruthenium(II) to yield the ruthenium metal complex B. The ^{1}H NMR and mass spectra were used to confirm the successful synthesis of the Schiff base ligand A and complex B. Biological activity and molecular docking studies were also investigated. The straightforward and convenient synthesis of this compound enables the construction of diverse chemical libraries, facilitating the discovery and development of potential bioactive molecules.

2.0. Materials and Methods

The carbonyl compound 4-hydroxybenzaldehyde and 3,3'-diaminobenzidine used for the synthesis of the tetraimine ligand were purchased from Sigma-Aldrich, Germany. Cis-

Dichlorobis(2,2′-bipyridine)ruthenium(II) was synthesized according to established procedures in the literature (Al-Wahaib et al., 2021). All reagents employed in the experiments were of analytical grade and used without purification. The solvents utilized in the study were obtained from Bristol Scientific, Nigeria. The deuterated solvents, which contain 0.03 vol% tetramethylsilane (TMS), were purchased from Merck. Nuclear magnetic resonance (NMR) spectra were recorded on a Varian Mercury XR300 (^{1}H: 300.08 MHz) spectrometer at the University of Cape Town, South Africa. Infrared (IR) absorptions were measured on a Perkin-Elmer Spectrum 100 FT-IR spectrometer. Mass spectrometry determinations were obtained using Electrospray Ionization (ESI) on a Waters API Quattro Micro triple quadrupole, with data recorded in positive ion mode. The culture media reagent used was nutrient agar. Ciprofloxacin 500 mg and ketoconazole 200 mg purchased were used as standard antibiotics.

2.1 Synthesis of tetraimine ligand

4-Hydroxybenzaldehyde (0.228 g, 1.87 mmol) was dissolved in methanol (25 mL), and 3,3'-diaminobenzidine (0.100 g, 0.467 mmol) was added and stirred. Five drops (catalytic amount) of acetic acid were added to the stirring solution (Scheme 1). The resulting yellow solution was stirred under reflux for 4 hours. The white precipitate formed was collected by suction filtration and washed with cold methanol and diethyl ether (20 mL). The product was purified by precipitation from hot methanol (20 mL). The resulting precipitate was filtered and dried *in vacuo*. The resulting ligand A is an off-white powder (Omosun & Smith, 2021).

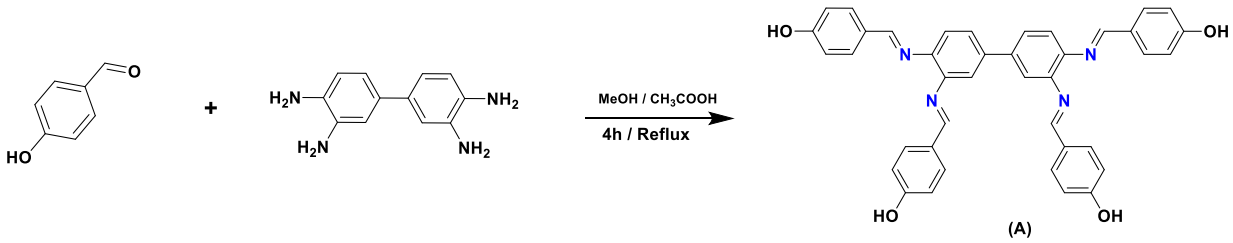

Scheme 1. Synthesis of the tetraimine ligand A.

2.2. Synthesis of diruthenium complex

The tetraimine ligand A (0.100 g, 0.158 mmol) was added to a stirring solution of cis-dichlorobis(2,2'-bipyridine)ruthenium (II) (0.154 g, 0.317 mmol) in ethanol (20 mL), and the mixture was refluxed for 4 hours (Scheme 2). The solvent from the reaction mixture was removed under reduced pressure using a rotary evaporator. The leftover residue was dissolved in water (30 mL) and partitioned with dichloromethane (60 mL) and diethyl ether (30 mL). The aqueous fraction was then concentrated to 3 mL under reduced pressure. A saturated aqueous solution of ammonium hexafluorophosphate (10 mL) was added, and the mixture was stirred for 30 minutes at room temperature. The precipitate was collected by vacuum filtration, washed with cold water (10 mL) and diethyl ether (15 mL), and dried *in vacuo*. The resulting product B is an orange powder (Motimani et al., 2022).

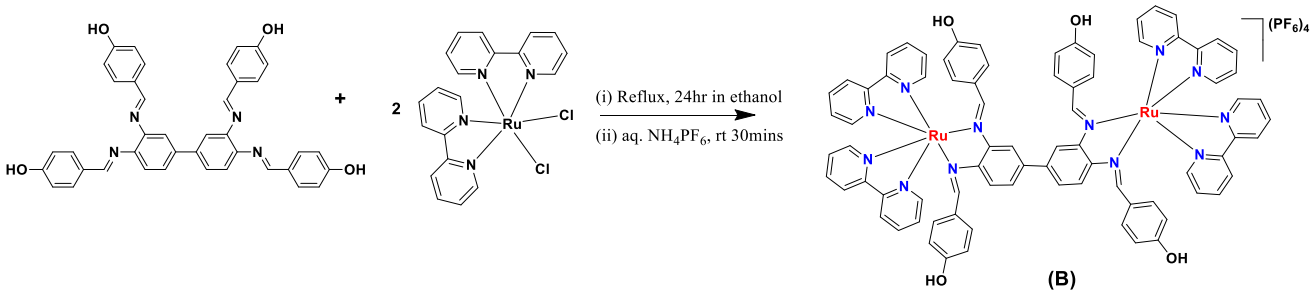

Scheme 2. Synthesis of tetraimine diruthenium complex B.

2.3. Microbial Assay

Inocula of five microbial strains were used to evaluate antimicrobial activity using a zone of inhibition assay. The microbial strains under this study included *Streptococcus pyogenes, Staphylococcus aureus (gram-positive bacteria), Escherichia coli, Proteus vulgaris (gram-negative bacteria),* and *Candida albicans*. These organisms were obtained from the Department of Microbiology, Michael Okpara University of Agriculture, Umudike, Abia State, Nigeria. Two concentrations (50 and 100 µg/mL) in dimethylformamide (DMF) were prepared from the complexes and tested against the strains. DMF was used as the negative control, and ciprofloxacin (50 µg/mL) as the positive control. In addition, Ketoconazole (50 µg/mL) was used as the reference antifungal agent. The biological activity of the tetraimine diruthenium complex was tested using the agar well diffusion method. Standard strains were first streaked at the surface of the agar, and a cork borer was used to create 5 wells, 2 cm apart, into the agar plates. The complexes and standard drugs were inoculated into their respective wells using a micropipette and were incubated at 35 °C for 24 hours for the bacterial strains and at the same temperature for 48 hours for the fungal strain. After the set incubation period, the diameters of the inhibition zones (mm) were recorded (Yakubu & Essel, 2025).

3.0. Results and Discussion

3.1. Synthesis and characterization of tetraimine ligand and diruthenium Complex

The tetraimine ligand A was synthesized *via* a Schiff base condensation reaction of the amine compound, 3,3'-diaminobenzidine, with the appropriate equivalent of 4-hydroxybenzaldehyde, following published literature methods (Omosun & Smith, 2021). Successful formation of the ligand was confirmed by ^{1}H NMR spectroscopy, as shown in Figure 1. All the expected aromatic proton signals corresponding to the structural features of the ligand were observed. Notably, the peaks associated with phenolic protons of the ligands appear as broad singlets at 9.96 and 9.40 ppm. Also, a distinct singlet assigned to the four imine protons appears at 5.51 ppm.

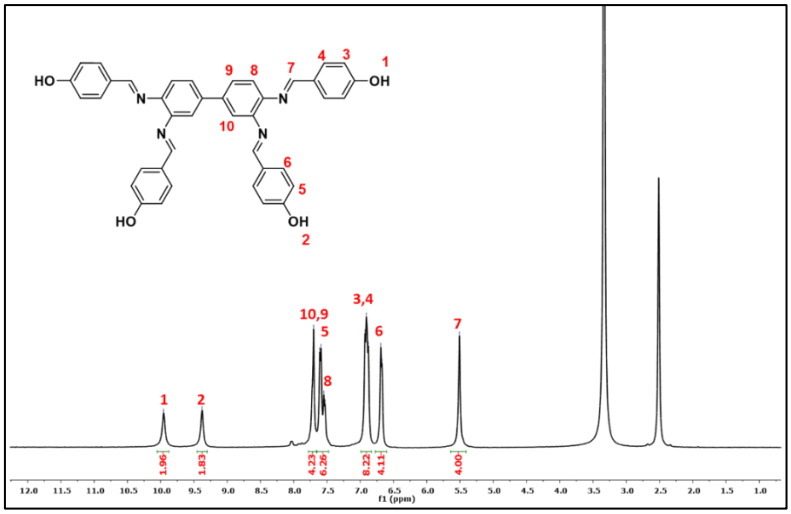

Figure 1: ^{1}H NMR spectrum of A in DMSO

HSQC (heteronuclear single quantum coherence) spectroscopy is a useful tool to observe one-bond correlations between carbons and protons (McKenzie et al., 2011). The successful Schiff-base synthesis (imine formation) was confirmed by HSQC, which showed a correlation between the key imine and the carbon-12 resonance signals, as shown in Figure 2 below. It clearly shows a cross-peak for this correlation, thus providing further evidence of successful Schiff-base formation.

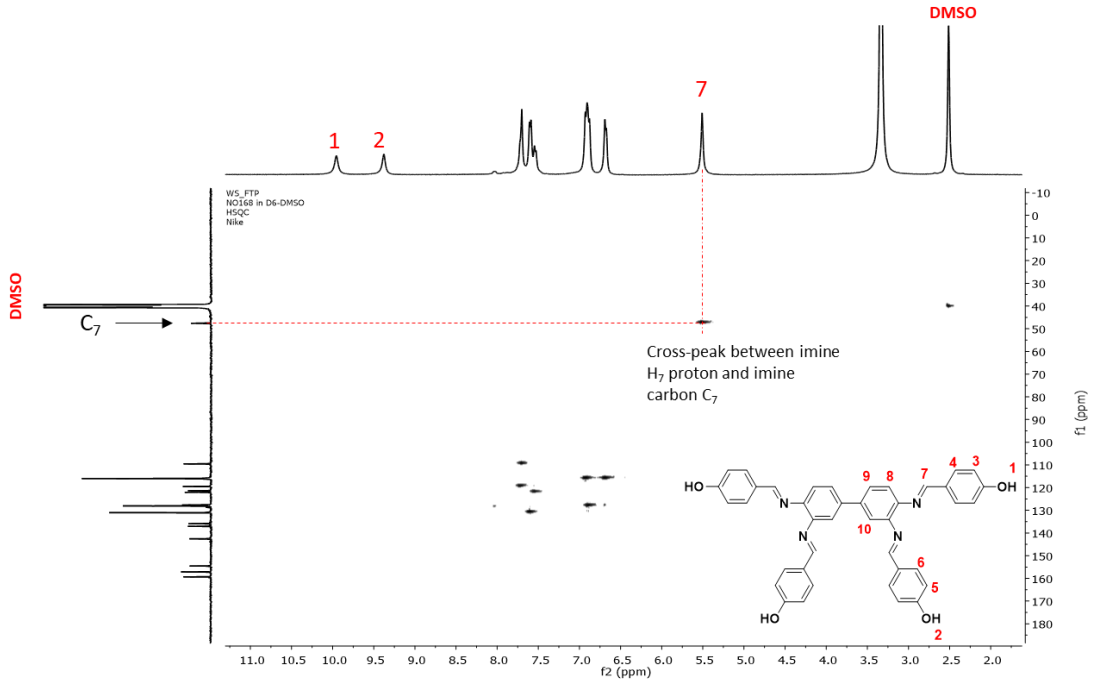

Figure 2: 2D NMR (HSQC) spectrum of A in DMSO

Complexation was achieved by reacting cis-dichlorobis(2,2'-bipyridine)ruthenium (II) metal precursor with the tetraimine ligand A in ethanol. The displacement of chloride from the reaction was facile using ammonium hexafluorophosphate, thus affording a new diruthenium cationic complex. Complex B was isolated in good yields, displaying solubility in chlorinated solvents, acetone, DMSO, and DMF.

The ^{1}H NMR spectrum of the diruthenium complex displays three overlapping multiplet signals in the aromatic region from 8.90 to 6.70 ppm, integrating for 54 protons (Figure 3). These signals are assigned to the C-H of the phenolic protons, phenyl rings of the tetraimine ligand, and bipyridine, proving successful formation of the compound and coordination of the metal precursor to the ligand.

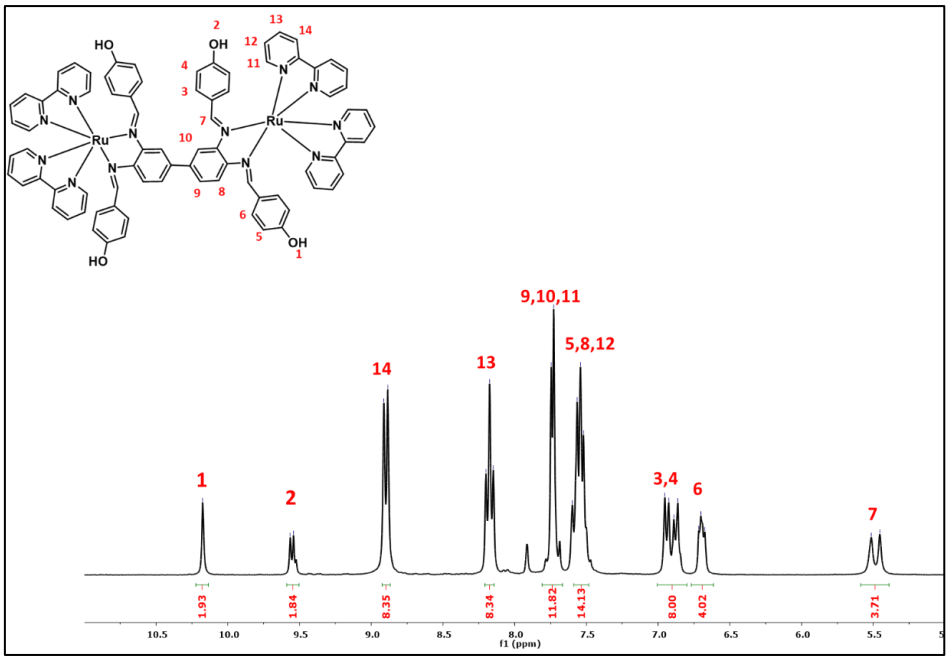

Figure 3: ^{1}H NMR spectrum of complex B in DMSO

The electron-withdrawing OH group of the phenolic protons is shown to appear downfield in the region of 10.18 – 9.55 ppm as two separate signals. This may be due to a cis or trans conformation or to an unsymmetrical para-substitution, leading to signals that resemble a pair of doublets. The imine proton signal in the NMR spectrum of complex B appears as a doublet. This could be attributed to spin-spin coupling between the imine proton and neighboring protons or, as previously suggested, to the non-equivalent cis and trans conformations, which have different chemical environments and lead to a splitting of the signal into two sub-peaks. In addition, the successful synthesis of the diruthenium complex B was evident by the appearance of signals corresponding to the bipyridyl protons when comparing the 1H NMR of the tetraimine ligand A and the diruthenium complex B, as shown in Figure 4.

The ^{13}C NMR spectrum of the complex shows the expected number of carbon signals consistent with the proposed molecular structure (Figure 5). The carbon signals for the phenolic moieties appear at 160.30, 158.40, 154.19, 142.51, and 137.15 ppm. The FT-IR spectroscopic result for the tetraimine ligand A displays a characteristic imine absorption band at 1607 cm^{-1}.

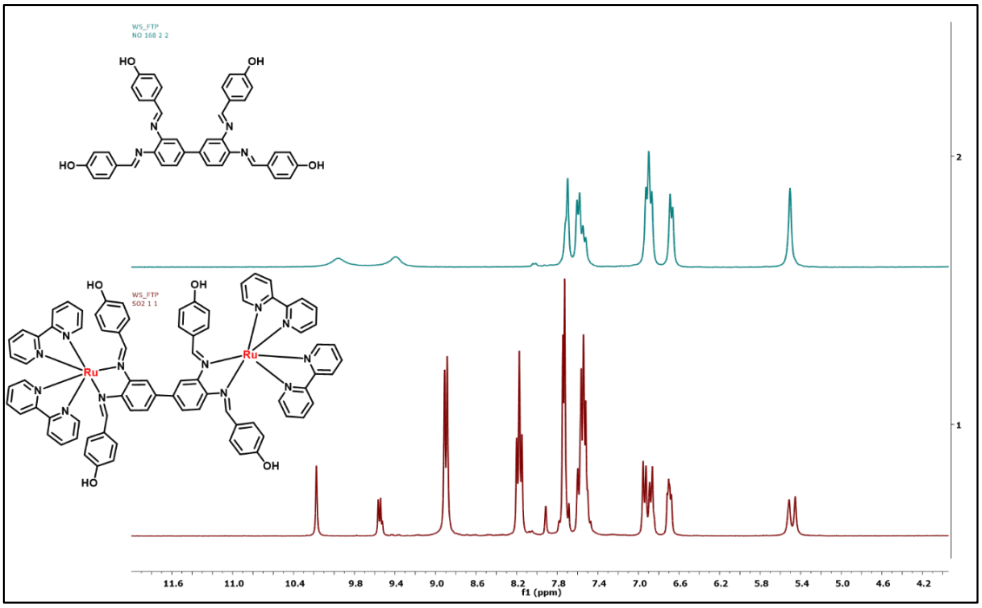

Figure 4: Stacked ^{1}H NMR spectra of ligand A and complex B in DMSO

In the FT-IR spectrum of complex B, a medium broad band at 3384.61 cm^{-1} for (O-H) was present. Furthermore, a shift in the C = N imine absorption bands to lower wavenumbers from 1607 cm^{-1} (metal-free ligand) to 1602 cm^{-1} was observed, as shown in Figure 6. This is ascribed to the back-bonding of the metal into the π∗(antibonding) orbitals of the imine, therefore increasing its electron density. This indicates that the tetraimine ligand is coordinated to metal centers. In addition, the high-resolution ESI-mass spectrum of B shows a base peak corresponding to the charged adduct $[M]^{+}$ at m/z = 1457.20, in the positive mode, as shown in Figure 7.

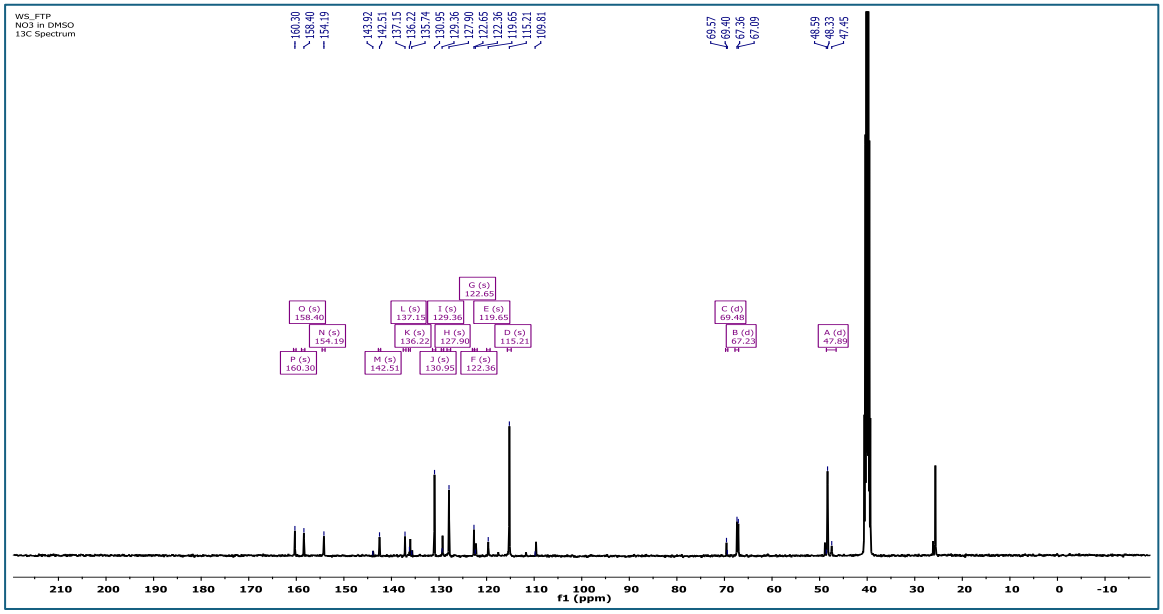

Figure 5: ^{13}C NMR spectrum of complex B

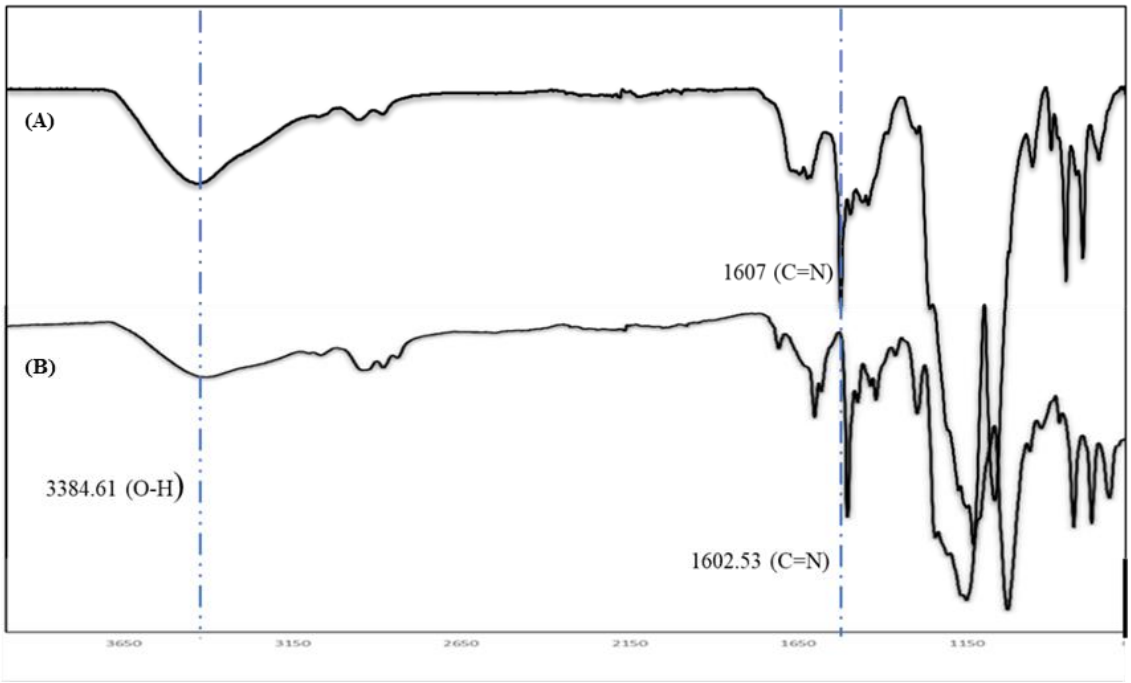

Figure 6: Stacked FT-IR spectra of ligand A and complex B.

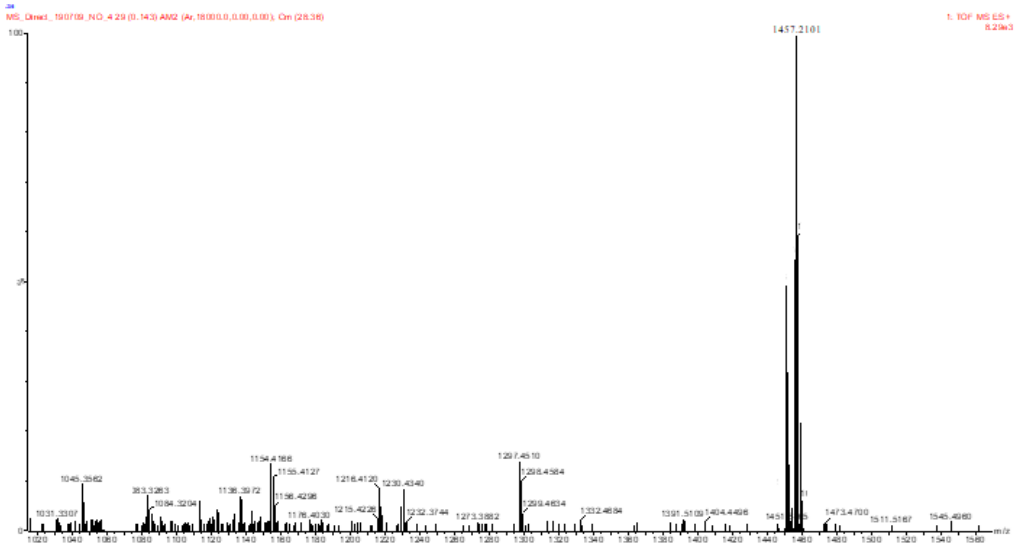

Figure 7: ESI-mass spectrum of complex B

3.2. Antimicrobial activity

The antimicrobial activity of the diruthenium complex was evaluated against selected bacterial and fungal strains using the zone-of-inhibition method and compared with its mononuclear derivative (Figure 8). This was done to determine whether increased nuclearity affects biological activity. The mononuclear complex was synthesized following a similar synthesis procedure to that of complex B. The results obtained for the mononuclear complex, binuclear complex, and standard drugs are presented in Table **1**. The antimicrobial potential was assessed at concentrations of 50 µg/mL and 100 µg/mL, while ciprofloxacin (50 µg/mL) and ketoconazole (50 µg/mL) served as reference antibacterial and antifungal drugs, respectively.

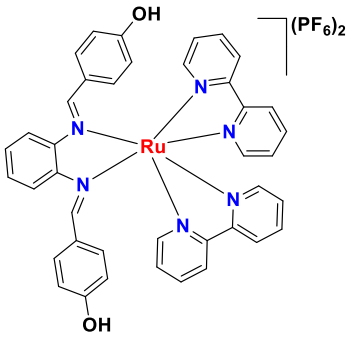

Figure 8: Structure of the mononuclear complex used for comparison

Table 1: Antifungal activities of binuclear complex in comparison with its mononuclear analog and standard drug. The diameter of zones of inhibition (mm).

Organisms	Mononuclear complex (µg/mL)		Binuclear complex (µg/mL)		Control (µg/mL)	
	50	*100*	*50*	*100*	Ciprofloxacin (50)	Ketoconazole (50)
S. pyogenes	8 ± 0.06	10 ± 0.05	11 ± 0.03	12 ± 0	14 ± 0.06	ND
S. aureus	8 ± 0	10 ± 0	13 ± 0.03	16 ± 0.03	16 ± 0.01	ND
E. coli	10 ± 0.14	11 ± 0.14	13 ± 0.06	15 ± 0.06	20 ± 0.01	ND
Proteus vulgaris	9 ± 0	10 ± 0.06	17 ± 0.03	22 ± 0.03	17 ± 0.05	ND
Candida albicans	-ve	-ve	-ve	11 ± 0	ND	18 ± 0.14

ND = Not detected

The results revealed that both complexes exhibited measurable antibacterial activity against all tested bacterial strains (*S. pyogenes, S. aureus, E. coli,* and *Proteus vulgaris*), though their effectiveness varied with concentration and complex type. In general, the binuclear complex demonstrated superior antimicrobial activity compared to the mononuclear analog, suggesting that metal nuclearity plays an important role in enhancing biological activity. At 50 µg/mL, the mononuclear complex showed relatively low antibacterial activity with inhibition zones ranging from 8–10 mm against the tested organisms. Upon increasing the concentration to 100 µg/mL, the inhibitory effect increased slightly, giving zones

between 10–11 mm, indicating a concentration-dependent response. However, these values were still significantly lower than those observed for the binuclear complex. In contrast, the binuclear complex exhibited markedly higher antibacterial activity. At 50 µg/mL, inhibition zones ranged from 11–17 mm, while at 100 µg/mL they increased further to 12–22 mm. Notably, the highest activity was observed against *Proteus vulgaris*, where the binuclear complex produced inhibition zones of 17 mm at 50 µg/mL and 22 mm at 100 µg/mL. These activities indicate that the binuclear complex possesses strong antibacterial potential, in some cases comparable to or exceeding that of standard antibiotics. For instance, against *Proteus vulgaris*, the binuclear complex at 100 µg/mL (22 mm) showed greater activity than ciprofloxacin (17 mm).

Despite these promising antibacterial results, the complexes demonstrated limited antifungal activity. The mononuclear complex showed no inhibitory effect against *Candida albicans* at both tested concentrations, whereas the binuclear complex exhibited activity only at the higher concentration of 100 µg/mL, with a zone of 11 mm. This value was considerably lower than the inhibition zone produced by the standard antifungal drug ketoconazole (18 mm), indicating that the synthesized complexes are less effective as antifungal agents.

The enhanced activity of the binuclear complex may be attributed to increased lipophilicity or improved affinity with microbial cell membranes, which can facilitate better penetration into microbial cells. Additionally, the presence of two metal centers may enhance the complex's ability to interact with vital cellular components such as proteins and nucleic acids, thereby hindering essential metabolic processes. The results show that binuclear complex **B** exhibits improved antibacterial activity compared to its mononuclear counterpart, particularly against Gram-negative bacteria such as *E. coli* and *Proteus vulgaris*. However, both complexes show relatively weak antifungal activity when compared with the standard antifungal drug. These findings highlight the potential of binuclear metal complexes as promising antibacterial agents and warrant further investigation into their mechanism of action and structural optimization.

3.3. SARS-CoV-2 molecular docking

Severe acute respiratory syndrome coronavirus 2 (SARS-CoV-2) is an enveloped, single-stranded RNA virus responsible for the coronavirus disease 2019 (COVID-19) pandemic. Viral replication and pathogenicity depend significantly on nonstructural protein 1 (NSP1), a key virulence factor that suppresses host gene expression by promoting degradation of host mRNA and interacting with the 40S ribosomal subunit. The three-dimensional crystal structure of NSP1 (**PDB ID: 7K3N**) is shown in Figure 9.

PatchDock server, a molecular docking algorithm based on shape complementarity principles, was used for docking analysis of ruthenium complexes to the SARS-CoV-2 nonstructural protein 1 (Schneidman-Duhovny et al., 2005). The NSP1 (PDB ID: 7K3N) of SARS-CoV-2 was downloaded from the RCSB Protein Data Bank. The water molecules were removed for clarity, and the structure of B was converted to PDB format using ArgusLab 4.0.1. In the PatchDock server, the complex was allowed to explore the entire surface of the target protein through blind docking. The PDB file of the complex, along with the protein structure, was uploaded to PatchDock for docking analysis.



Figure 9: The 3D crystal structure of the Nonstructural protein 1 (NSP1) (PDB ID: 7K3N)

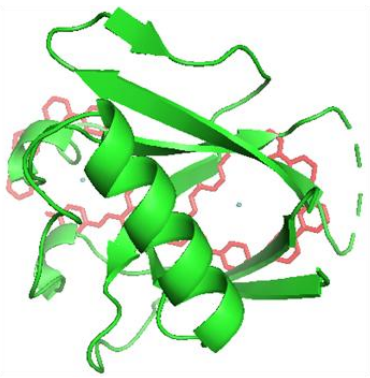

Figure 10: Docked solutions of binuclear ruthenium(II) complex with NSP1 of SARS-CoV-2 Global energy = -18.35 Kcal/mol

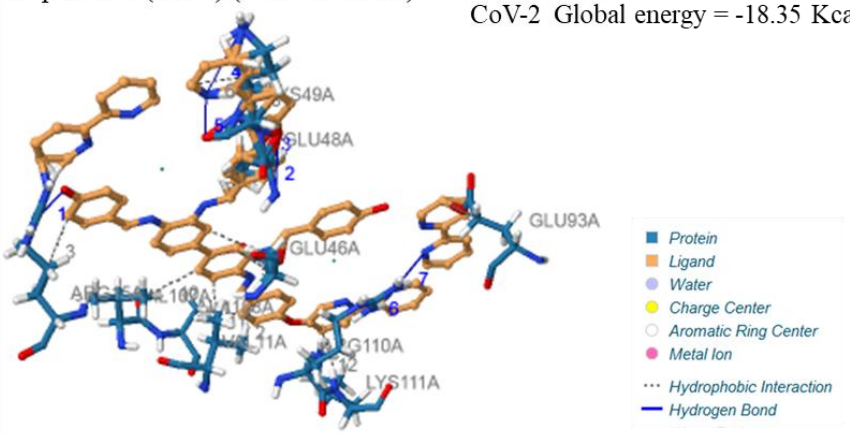

Figure 11: Protein ligand interaction of dinuclear ruthenium (II) complex with NSP1 of SARS-CoV-2, visualized using PLIP server

The default cluster RMSD value of 4.0 Å and the protein-small-ligand complex option were used as docking parameters. The top-ranked docking solutions, as shown in Figure 10, were obtained from PatchDock and were further refined using the FireDock server (Mashiach et al., 2008).

The resulting docked conformations were visualized using PyMOL and analyzed with the Protein–Ligand Interaction Profiler (PLIP) server (Khater & Nassar, 2021). Analysis of the protein–ligand interactions between the binuclear ruthenium complex and NSP1 of SARS-CoV-2 (Figure 11) revealed the presence of both hydrophobic interactions and hydrogen bonds. Hydrophobic interactions were observed with the following protein residues: VAL11A (2.66 Å), VAL11A (3.82 Å), ARG15A(3.84 Å), GLU46A(3.38 Å), GLU46A(2.49 Å), LYS49A(2.85 Å), LYS49A (1.13 Å), LYS49A (1.31 Å), GLU93A (3.66 Å), VAL107A (3.34 Å), ALA108A (2.53 Å) and LYS111A (3.19 Å). Hydrogen bonds were observed with protein residues ARG15A (1.47 Å), GLU48A (2.16 Å), GLU48A (2.84 Å), LYS49A (2.80 Å), LYS49A (2.11 Å), ARG110A (2.06 Å) and ARG110A (2.09 Å), The global energy (binding energy) value of -18.35 Kcal/mol suggested that the binuclear ruthenium (II) complex is a potential drug candidate against SARS-CoV-2.

4.0. Conclusions

A novel ruthenium complex based on a tetraiimine ligand was successfully synthesized and characterized using various spectroscopic techniques. Antimicrobial evaluation using the agar well diffusion method revealed significant activity against *Candida albicans, Escherichia coli, Staphylococcus aureus, Proteus vulgaris,*

and Streptococcus pyogenes. It was found that the binuclear complex exhibited greater antibacterial activity than its mononuclear derivative. Molecular docking studies targeting the non-structural protein 1 NSP1 of SARS-CoV-2 suggested that the ruthenium complex may have potential as a therapeutic candidate against SARS-CoV-2 infection. This is consistent with prior literature (Roy et al., 2023; Nwankwo et al., 2022; Otuokere et al., 2022). However, further *in vitro, in vivo,* and clinical investigations are necessary to fully establish the compound's efficacy and safety as an antimicrobial and antiviral agent.

References

Afrin, D. S., Farhana, A. B., Md Saddam, H. B., Nuruzzaman, K. M., Kudrat-E-Zahan, B., & Md Mahasin, A. B. (2018). A short review on chemistry of schiff base metal complexes and their catalytic application. *International Journal of Chemical Studies*., *6*(3): 2859–2866.

Ahmed, S. K., Hussein, S., Qurbani, K., Ibrahim, R. H., Fareeq, A., Mahmood, K. A., & Mohamed, M. G. (2024). Antimicrobial resistance: Impacts, challenges, and future prospects. *Journal of Medicine, Surgery, and Public Health*, *2:* 100081.

Al-Wahaib, D., El-Dissouky, A., Abrar, N. M., & Khalil, T. E. (2021). Synthesis, characterization, and antimicrobial activity investigations of ruthenium (II)–bipyridine complexes of ciprofloxacin derivatives. *Applied Organometallic Chemistry*, *35*(11): 6407.

Antony, A. M., & Patil, S. A. (2024). Review: Diverse biomedical applications of imine-based metal complexes derived from 2-hydrazinobenzothiazole. *Journal of Coordination Chemistry*, 77(19): 1994–2017.

Babgi, B. A., Domyati, D., Abdellattif, M. H., & Hussien, M. A. (2021). Evaluation of the Anticancer and DNA-Binding Characteristics of Dichloro(diimine)zinc(II) Complexes. *Chemistry*. *3*(4): 1178–1188.

Balachandran, G., Dhamotharan, A., Kaliyamoorthy, K., Rajammal, K. S., Kulandaiya, R., & Raja, A. (2024). Synthesis, Characterization, and Catalytic Applications of Schiff-Base Metal Complexes. *Engineering Proceedings.* 61(1): 26.

Catalano, A., Sinicropi, M. S., Iacopetta, D., Ceramella, J., Mariconda, A., Rosano, C., Scali, E., Saturnino, C., & Longo, P. (2021). A review on the advancements in the field of metal complexes with schiff bases as antiproliferative agents. *Applied Sciences,*. 11(13): 6027.

Clemente, M., Polat, I. H., Albert, J., Bosque, R., Crespo, M., Granell, J., López, C., Martínez, M., Quirante, J., Messeguer, R., Calvis, C., Badía, J., Baldomà, L., Font-Bardia, M., & Cascante, M. (2018). Platinacycles Containing a Primary Amine Platinum(II) Compounds for Treating Cisplatin-Resistant Cancers by Oxidant Therapy. *Organometallics*, 37(20): 3502–3514.

Dini, I. (2026). Mechanisms of Bacterial Resistance and Innovative Strategies to Overcome Antimicrobial Resistance. *Antibiotics,* 15(3): 319.

Gaber, A., Belal, A. A. M., El-Deen, I. M., Hassan, N., Zakaria, R., Alsanie, W. F., Naglah, A. M., & Refat, M. S. (2021). Synthesis, spectroscopic characterization, and biological activities of new binuclear co(ii), ni(ii), cu(ii), and zn(ii) diimine complexes. *Crystals*, 11(3): 300.

Gonzalez-Oñate, A., Chaparro, D., Quevedo, R., Alí-Torres, J., & Flores-Gaspar, A. (2026). NMR spectroscopic and computational analysis of E/Z isomerism in imines derived from isatin. *RSC Advances*, *16*(14): 12238–12245.

Govender, P., Therrien, B., & Smith, G. S. (2012). Bio-metallodendrimers - Emerging

strategies in metal-based drug design. *European Journal of Inorganic Chemistry*, 2012 (17): 2853–2862.

Iacopetta, D., Ceramella, J., Catalano, A., Saturnino, C., Bonomo, M. G., Franchini, C., & Sinicropi, M. S. (2021). Schiff bases: Interesting scaffolds with promising antitumoral properties. *Applied Sciences,* 11(4): 1877.

Jean-Baptiste, K. N., Guillaume, K. C., Claude, K. A. L., Witabouna, K. M., Ahoua, A. R. C., & Nahosse, Z. (2017). Synthesis, Characterization and Antimicrobial Evaluation of Symmetric A-Diimine Schiff Bases Derived from Cis and Trans Racemic Mixture of Cyclohexanediamine. *IRA-International Journal of Applied Sciences*, 6(1): 23.

Kathiresan, S., Mugesh, S., Annaraj, J., & Murugan, M. (2017). Mixed-ligand copper(II) Schiff base complexes: the vital role of co-ligands in DNA/protein interactions and cytotoxicity. *New Journal of Chemistry*. 41(3): 1267–1283.

Khater, I., & Nassar, A. (2021). Repurposing Antiviral Drugs to Inhibit SARS-CoV-2 Papin-Like Protease Activity. *International Journal of Intelligent Computing and Information Sciences*, 21(1): 149–164.

Mashiach, E., Schneidman-Duhovny, D., Andrusier, N., Nussinov, R., & Wolfson, H. J. (2008). FireDock: a web server for fast interaction refinement in molecular docking. *Nucleic Acids Research*, 36(1): 229–232.

McKenzie, J. S., Donarski, J. A., Wilson, J. C., & Charlton, A. J. (2011). Analysis of complex mixtures using high-resolution nuclear magnetic resonance spectroscopy and chemometrics. *Progress in Nuclear Magnetic Resonance Spectroscopy*, 59(4): 336–359.

More, V. S., Chumbhale, D. C., Rangari, N. T., Mishra, P. A., Jagnar, A. B., & Kadam, J. N. (2022). Synthesis, analgesic and anti-inflammatory activities of some pyrazolo[3,4-c]pyrazole derivatives. *International Journal of Health Sciences*, 6(2): 1218–1231.

Motimani, N. M., Ngubane, S., & Smith, G. S. (2022). Polynuclear heteroleptic ruthenium(II) photoredox catalysts: Evaluation in blue-light-mediated, regioselective thiol-ene reactions. *Polyhedron*, 212: 115616.

Nastasi, F., La Ganga, G., Di Pietro, M. L., Serroni, S., Campagna, S., & Puntoriero, F. (2022). Multinuclear Metal Complexes: Coordination Dendrimers, Polymers, and Coordination Cages. *Springer Handbooks*, 643–689.

Nwankwo CI, Omeh YN, Omodamiro OD, Otuokere IE, Alaebo PO, Atasie OC, Ekwuribe GA (2022). Phenolics of *Abelmoschus esculentus* pods: HPLC identification and in silico studies to identify potential anti-inflammatory agents. *Journal of Natural Product Research,* 6(8):1311–1319.

Omosun, N. N., & Smith, G. S. (2021). Monometallic and bimetallic sulfonated Rh(I) complexes: Synthesis and evaluation as recyclable hydroformylation catalysts. *Journal of Organometallic Chemistry*, 951: 122022.

Otuokere IE, Akoh OU, Echeme JO, Nwadire FC, Nwankwo CI, Egbucha JN, Ammasai K. (2022). GC-MS analysis and molecular docking studies to identify potential SARS-CoV-2 nonstructural protein inhibitors from Icacina trichantha Oliv tubers. *Journal of Natural Product Research,* 6(8):1336–1342.

Roy R, Sk MF, Tanwar O, Kar P. (2023). Computational studies indicated the effectiveness of human metabolites against SARS-Cov-2 main protease. *Molecular Diversity*, 27(4):1587-1602

Schneidman-Duhovny, D., Inbar, Y., Nussinov, R., & Wolfson, H. J. (2005). PatchDock and SymmDock: Servers for

rigid and symmetric docking. *Nucleic Acids Research*, 33(2), 363–367.

Waters, J. E., Stevens-Cullinane, L., Siebenmann, L., & Hess, J. (2023). Recent advances in the development of metal complexes as antibacterial agents with metal-specific modes of action. *Current Opinion in Microbiology*, 75: 102347.

Yakubu, A., & Essel, G. K. (2025). Preliminary evaluation of the phytochemical constituents and anti-microbial activity of leaf extracts of Rhexia virginica plant. *The Pharma Innovation Journal*, 14(5),103–110.